applied sciences

MDPI

Review

Lamellar MWW-Type Zeolites: Toward Elegant Nanoporous Materials

Anderson Schwanke [1,*] and Sibele Pergher [2]

[1] Instituto de Química, Laboratório de Reatividade e Catálise, Universidade Federal do Rio Grande do Sul, Porto Alegre 91540-000, RS, Brazil

[2] Instituto de Química, Laboratório de Peneiras Moleculares (LABPEMOL), Universidade Federal do Rio Grande do Norte, Natal 59078-970, RN, Brazil; sibelepergher@gmail.com

* Correspondence: anderson-js@live.com; Tel.: +55-54-98129-3396

Received: 11 July 2018; Accepted: 7 August 2018; Published: 13 September 2018

Featured Application: This work is a compilation of different strategies to obtain lamellar zeolitic materials with a hierarchical structure of pores. The aim of this work is to offer a greater dissemination of MWW-type lamellar zeolites to demonstrate the most recent strategies for obtaining materials with different pore architectures and providing promising applications in catalysis, adsorption, and separation.

Abstract: This article provides an overview of nanoporous materials with MWW (Mobil twenty two) topology. It covers aspects of the synthesis of the MWW precursor and the tridimensional zeolite MCM-22 (Mobil Composition of Matter number 22) as well as their physicochemical properties, such as the Si/Al molar ratio, acidity, and morphology. In addition, it discusses the use of directing agents (SDAs) to obtain the different MWW-type materials reported so far. The traditional post-synthesis modifications to obtain MWW-type materials with hierarchical architectures, such as expanded, swelling, pillaring, and delaminating structures, are shown together with recent routes to obtain materials with more open structures. New routes for the direct synthesis of MWW-type materials with hierarchical pore architecture are also covered.

Keywords: zeolite; MWW; MCM-22; hierarchical zeolite; lamellar zeolite; layered zeolite; two-dimensional zeolites; swelling; pillaring; delaminating

1. Introduction

Zeolites are a class of crystalline materials formed by a skeleton based on tetrahedral silicon and aluminum (and others, such as P, Ge, Ga, B, S, and Fe), which form microporous (<2 nm) channels and cavities. Due to their microporous structure, these materials are extremely versatile and are widely used as adsorbents, ion exchangers, detergents, and catalysts [1–3]. However, it is in the catalysis field that zeolites play an essential role in refining, processing, and organic synthesis for fine chemistry. In fact, zeolites make up more than 40% of the solid catalysts used in the chemical industry [4].

In the last two decades, two-dimensional lamellar zeolitic precursors (LZPs) have been found for some types of zeolites. These LZPs show the same basic structure as the tridimensional form with separated lamellae approximately 1 to 2 nm thick along one direction, and these precursors condense topotactically, producing three-dimensional structures. According to the International Zeolite Association (IZA), there are more than 200 framework topologies, and less than 10% of these structures have an LZP or exist in a two-dimensional form [5]. MWW, FER, NSI, OKO, RRO, CAS, CDO, PCR, RWR, and AFO are some examples of zeolite framework topologies that exist with a lamellar form. Readers can find the list of lamellar zeolites and their references in excellent reviews [6–10].

Among these framework topologies, LZP with MWW topology, known as (P)MCM-22 (MCM-22 precursor), is remarkably the most studied LZP. Moreover, its modification with postsynthetic procedures yields engineered materials with different pore architectures and lamellae organizations, such as hybrid organic-inorganic, pillared, misaligned, disordered, delaminated, and desilicated structures [11]. These modifications open avenues to obtaining elegant and designed solids with hierarchical pore structures that could facilitate reactants in reaching active sites to increase the conversion and yield of the desired products. Considering the importance and the versatility of this class of nanoporous materials, this work will focus on MWW-type zeolites, showing their general aspects of synthesis and recent advances.

2. The Precursor (P)MCM-22 and MCM-22 Zeolites

(P)MCM-22 was reported in 1990 by Mobil and is composed of individual lamellae with a thickness of 2.5 nm, with sinusoidal 10-ring channels (0.40 × 0.50 nm) and 12-ring hemicavities (connected to each other by double 6-rings with an aperture of ~0.3 nm) on the upper and lower surface of the lamella [12,13]. The precursor contains hexamethyleneimine (HMI) molecules used as a structure directing agent (SDA) occluded in the sinusoidal channels, as shown in Figure 1a. The interaction between lamellae occurs via hydrogen bonds between silanol groups on the surface and the HMI molecules also present between the MWW lamellae [8].

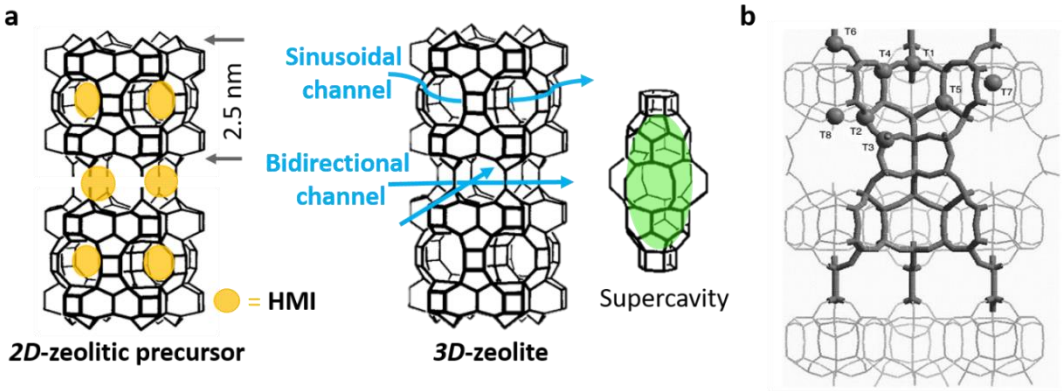

Figure 1. The two-dimensional (2D) zeolitic precursor and three-dimensional (3D) MWW (Mobil twenty two) zeolitic structure (**a**); its eight different tetrahedral sites (**b**); HMI (hexamethyleneimine). Adapted from Reference [14,15]. Copyright (1998), with the permission of the Royal Society of Chemistry, and Copyright (2006), with permission from Elsevier.

After calcination, the organic content is removed and the silanol groups between lamellae are condensed to form three-dimensional MCM-22 zeolite, as shown in Figure 1a. Consequently, an additional two-directional 10-ring (0.40 × 0.55 nm) channel, formed as the union of 12-ring hemicavities, generates internal super cages (free internal diameter of 0.71 nm and internal height of 1.82 nm), which are also connected to the aforementioned two-directional 10-ring channels [13]. In addition, it is possible to obtain a three-dimensional MCM-22 analog called MCM-49, which is obtained by direct crystallization by increasing the relative proportion of alkali in the gel composition [16]. Furthermore, another material called MCM-56 with a partial disorder of lamellar stacking is obtained when the reaction to form MCM-49 is stopped in the middle of the crystallization course [17,18].

The MCM-22 zeolite with high crystallinity can be obtained with Si/Al molar ratios between 15 and 70 (usually 20). However, ferrierite competing phases are found when the amount of aluminum increases (Si/Al = 9), as shown in the microscopic analysis of Figure 2 (image a, white arrows). In contrast, the decrease in aluminum in the synthesis gel (Si/Al > 70) leads to MFI (Mobil Five) competing phases [19]. It is also possible to obtain a pure silica zeolite MCM-22 analog by direct

synthesis using mixtures of trimethyladamantylammonium ($TMAda^+$) and HMI as a second organic template, which is known as ITQ-1 [14].

The Si/Al ratio associated with the synthesis temperature and the static and dynamic (rotation of the autoclaves) conditions of the gel aging could interfere in the formation of MCM-22. It was reported that the use of 30 < Si/Al < 70 and temperatures above 150 °C results in the formation of ferrierite and/or mordenite competing phases. At temperatures below 150 °C with dynamic conditions, the MCM-22 phase is insignificant, while the formation of other phases increases with a decrease in the Si/Al ratio [20]. Other authors have reported that an MCM-22 formation with no other phase competitions was avoided using temperatures between 135 and 150 °C. Furthermore, dynamic conditions produce MCM-22 zeolite with good quality, while static conditions result in the nonsignificant formation of the desired phase or even the formation of pure ferrierite [20,21]. In addition, it was reported that the previous aging of the gel at 180 °C for 4–12 h and static conditions produced pure MCM-22 with a reduced crystallization time [22].

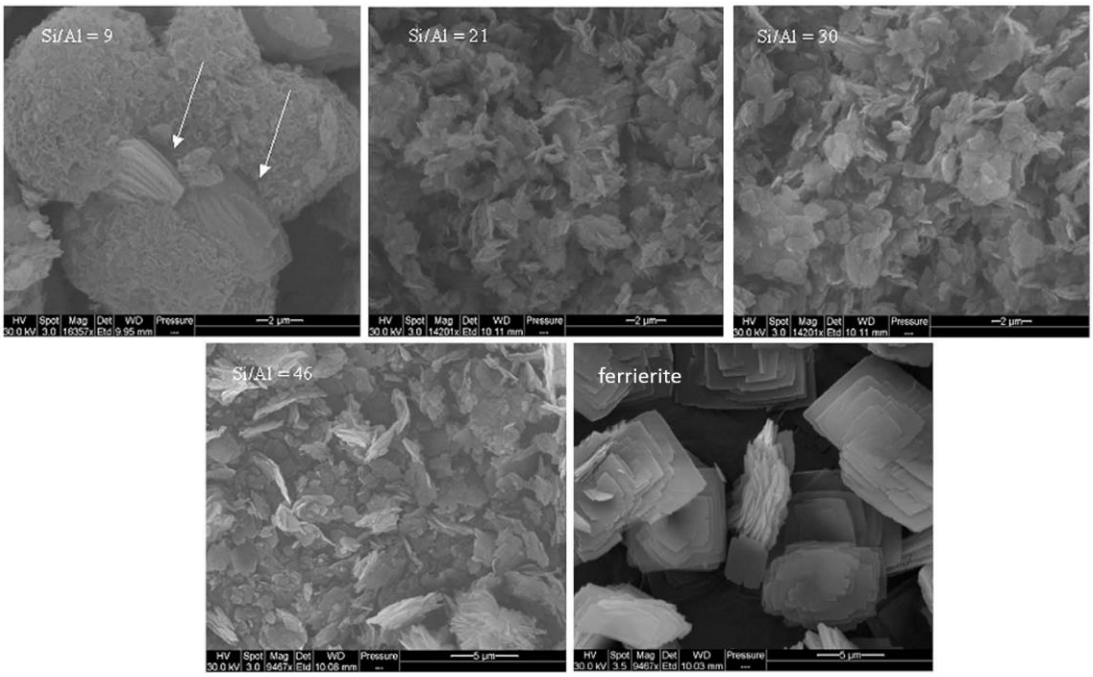

Figure 2. Morphologies of MCM-22 with different Si/Al molar ratios = 9, 21, 30, 46. The last image corresponds to pure ferrierite formed under static conditions. Adapted from Reference [19]. Copyright (2009), with permission from Elsevier.

MCM-22 presents distinct acid sites that reveal the homogeneity in acid strength. The microcalorimetry results showed a concentration of acid sites (for an MCM-22 with Si/Al = 16) of 1052 $\mu mol \cdot g^{-1}$, which is modestly higher than the concentration of aluminum ions, 947 $\mu mol \cdot g^{-1}$, suggesting that all aluminum ions produce acid sites either by producing an unbalanced charge structure that is balanced by the proton or active as Lewis acid sites. It was assumed that the aluminum ions in the zeolite structure do not act as Lewis acid sites because they are "protected" by nearby protonic centers. These aluminum ions may be located on the extra-framework where the structure is relaxed, acting as Lewis acid sites. The author of this study pointed out that the additional concentration of acid sites (105 $\mu mol \cdot g^{-1}$) may be related to silanol groups located at the external surface [23].

Studies employing infrared spectroscopy with adsorbed pyridine have reported that for samples with Si/Al = 10, 14, and 30, most acid sites (50–70%) are located in the supercavities. The other sites are located in the sinusoidal channels (20–30%) or connected to the hexagonal prisms between supercavities, with values of 10% for Si/Al = 10 and 14 and 20% for Si/Al = 30 [24]. In addition,

a study using density functional theory reported that the favorite placement sites of aluminum ions are the sites T1, T3, and T4, as shown in Figure 1b. The T2 site is presented as less favorite and the acidity of the T1 and T4 sites are equivalent and stronger than that of the T3 site, respectively [15].

Regarding the good performance of the MWW materials for benzene alkylation reactions, and despite the small size of the channel apertures, it is suggested that a significant number of cavities are open on the surface of the crystallites. It was assumed that the "cups" of the supercavities have a free diameter of 0.71 nm and the formation of cumene and ethylbenzene must occur in these cavities without any diffusional barrier. This hypothesis is supported when catalytic activity is significantly decreased by deactivation with 2,6-di-tert-butylpyridine, a large molecule that cannot enter in the channels of MCM-22. However, spectroscopic results confirm that benzene could easily enter the supercavities [23,25].

The hydrothermal crystallization and morphology of MCM-22 can be significantly altered by static or dynamic conditions. The dynamic condition minimizes the excessive aggregation of the crystals (see Figure 3a) when compared with static conditions, as shown in Figure 3b–g. Synthesis under dynamic conditions also induces the formation of zeolite with a higher crystallinity in a shorter time [17].

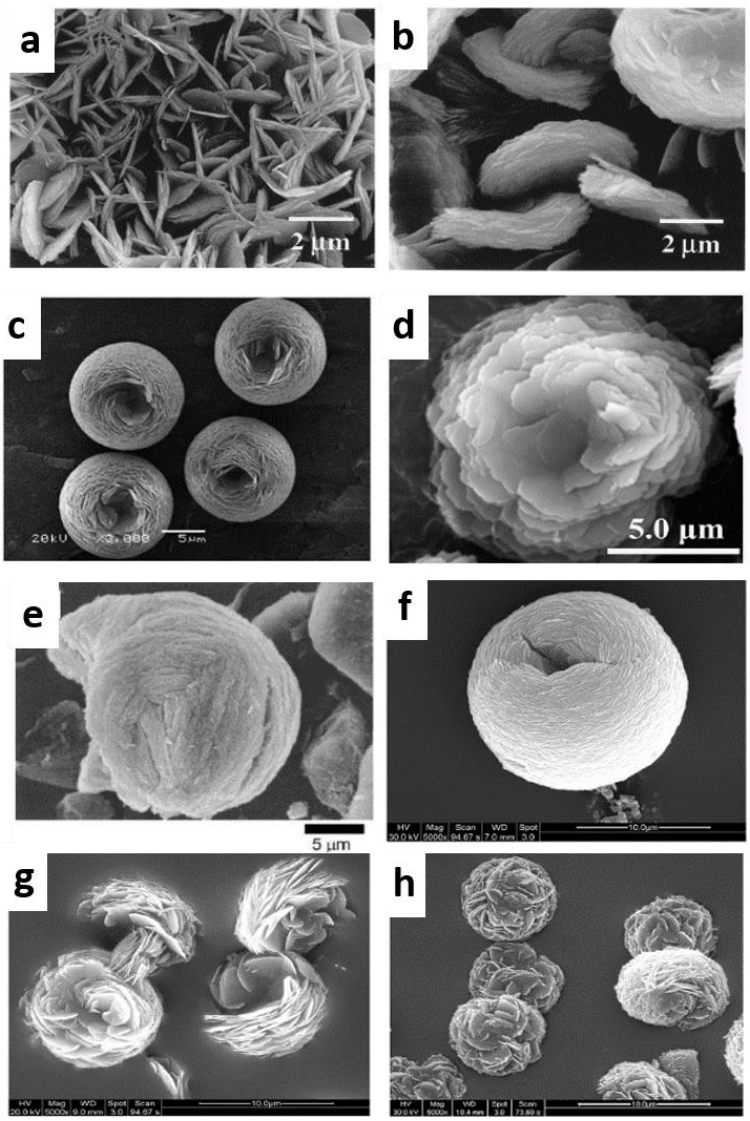

Figure 3. Morphologies of MCM-22 zeolites obtained under dynamic (**a**) and static conditions (**b**–**h**). The zeolites under static conditions differ in methodology, molar composition, silicon source, and temperature. Adapted from Reference [9,26–29].

The crystallization of MCM-22 is also influenced by the source of silicon used because its degree of dissolution affects nucleation and crystal growth. A study compared three silicon sources with different surface areas: silicic acid (750 $m^2 \cdot g^{-1}$), silica gel (500 $m^2 \cdot g^{-1}$), and precipitated Ultrasil silica (176 $m^2 \cdot g^{-1}$); zeolite with 100% crystallinity was obtained with silicic acid followed by silica gel (90%) and Ultrasil (80%) by aging the gel for 7 days in dynamic conditions [26]. The authors showed high crystallinities obtained under static conditions using silicic acid when compared with the other silicon sources. This indicates that silicon sources with a high surface area are a determining factor in the crystallization of MCM-22. Figure 3a,b show the morphologies of materials synthesized with silicic acid.

Other sources of silicon were used, such as sodium metasilicate, water-glass, and colloidal silica [29]. The use of sodium metasilicate reduced the induction period (less than 12 h) with a crystallized product after 6 days. Colloidal silica and water-glass required induction periods of 2 and 2.5 days, respectively. These differences were attributed to the different dissolution rates of each silicon source. The morphologies of zeolites synthesized with colloidal silica, sodium metasilicate, and water-glass are shown in Figure 3 (images f–h, respectively).

The use of silicon alkoxide as tetraethyl orthosilicate (TEOS) for the synthesis of MCM-22 has been reported [27]. The methodology involves a first step of pre-hydrolysis of TEOS catalyzed with a strong acid media (pH ranging from 0.98–1.65), followed by a second step of hydrothermal reaction of the hydrolyzed precursor with HMI and a source of aluminum in a base media with a pH value ranging from 11–12. This allows a shorter crystallization time, which differs from traditional methods where hydrolysis, condensation, and crystallization occur simultaneously in the same basic medium. According to the authors, MCM-22 with a crystallinity of 98% was produced after 3 days at 158 °C. Figure 3d shows the morphology of the obtained product.

Silica from burned rice husks was used to synthesize MCM-22 [30]. X-ray diffraction analysis confirmed that the product has an MWW structure and textural analysis showed a surface area of 384 $m^2 \cdot g^{-1}$ and a pore volume of 0.28 $cm^3 \cdot g^{-1}$. Microscopic analysis showed different particles with interrupted growths, spherical aggregates, and concentric rings.

Structure Directing Agent (SDA)

The design of SDA for the synthesis of zeolites is a subject of continuous research and, for the MWW topology, it is possible to synthesize different materials with other SDAs than HMI. Here, the use of different SDAs is organized in chronological order.

1987—An aluminosilicate-based material was discovered, named SSZ-25, which exhibited the same characteristics as MWW materials [31]. However, it was initially assumed that the material only had 12-ring channels. Subsequently, it was confirmed that the structure of SSZ-25 was isomorphic to the structure of PSH-3 previously synthesized with HMI three years prior [32]. In this case, *N*,*N*,*N*-trimethyl-1-adamantyl ammonium hydroxide ($TMAda^+OH^-$) was used as an SDA.

1988—A material called ERB-1 was reported, which was the first LZP where aluminum and boron were tetrahedrally coordinated into the MWW structure and piperidine was used as an SDA, and the use of alkali cations was not necessary [33].

1998—$TMAda^+OH^-$ was also used to obtain ITQ-1, a pure silica zeolite. To obtain this material, mixtures of $TMAda^+OH^-$ with HMI had a particular role in the synthesis because $TMAda^+OH^-$ allowed the formation of the external 12-ring hemicavities and HMI contributed to the stabilization of the sinusoidal 10-ring channels present in the internal structure of the MWW lamella [14].

2004—The use of diethyldimethylammonium (DEDMA), ethyltrimethylammonium (ETMA), or hexamethonium (HM) cations as the SDA were reported, and the obtained material was called UZM-8 [34]. UZM-8 was synthesized with a Si/Al molar ratio between 6.5 and 35 and a disordered lamellar structure similar to that of MCM-56 zeolite.

2006—The use of *N*-methylsparteinium (MSPT) as an SDA in a high-throughput synthesis led to the discovery of ITQ-30, an MWW-type zeolite with disordered lamellae similar to MCM-56 [35].

2011—The use of (bis(*N*,*N*,*N*-trimethyl)-1,5-pentanediaminium dibromide as an SDA was reported and conducted to form an EMM-10 precursor [36]. The material is similar to (P)MCM-22, but its lamellae are vertically misaligned.

2013—The use of 1,3-diisopropylimidazolium, a 1,3-diisobutylimidazolium cation, and 1,3-dicyclohexylimidazolium cations were reported to obtain a zeolite named SSZ-70 [37].

2015—A new synthesis of MWW-type materials was reported. It employed 1,3-bis (cyclohexyl)imidazolium hydroxide (IM^+OH^-) as an SDA, and the obtained materials were called ECNU-5A and ECNU-5B [38]. The procedure used calcined ITQ-1 as a silica source, which was recrystallized with an aqueous solution containing IM^+OH^-. The crystals of MWW rapidly dissolved due to the high basic pH in only 1 h at 170 °C, yielding only 17.8% and increasing to 92.3% after 24 h. The obtained materials showed a horizontal displacement with misaligned MWW lamellae structure in ABAB or ABC stacking sequence, caused by the geometry between IM^+OH^- and the silica structure.

The use of aniline (AN) with mixtures of HMI for the synthesis of MWW zeolites was reported [39,40]. In this case, AN acts as a structure-promoting agent via space filling, and the authors pointed out that the use of AN contributed to the formation of the zeolitic structure because the molecules were not trapped within the MWW structure. Moreover, its recovery and recycling may contribute to low-cost synthesis.

2017—1-adamantanamine as an SDA was reported and the obtained material, called ECNU-10, had a three-dimensional structure analogous to MCM-49 zeolite [41]. ECNU-10 could be obtained when the gel Si/Al ratio was 12–13.5 in a relatively narrow phase region.

2018—A direct synthesis of three-tridimensional MCM-49 using cyclohexylamine (CHA) as an SDA was reported [42]. CHA has a low toxicity and low cost and the obtained results showed that more CHA molecules occupy the hemicavities on the surface and the supercavities, and the SiO_2/Al_2O_3 ratio of the obtained product could be up to 34.6. The authors compared the products synthesized with CHA or HMI for the liquid phase alkylation of benzene with ethylene and similar catalytic performances were observed.

3. MWW-Type Materials by Post-Synthesis Modifications

(P)MCM-22 offers diverse possibilities to obtain more open structures. The first example of this is the interlayer expanded zeolite called IEZ-MWW, in which silanol groups of the LZP were reacted with alkoxysilanes such as $SiMe_2Cl_2$ or $Si(EtO)_2Me_2$ [43]. After calcination, a 12-ring pore was formed by the single silicon atoms that act as small pillars, as represented in Figure 4. The increase in pore structure may serve catalytic purposes to diffuse large molecules and as selective adsorbents for adsorption and separation.

The successful swelling procedure is a key step to obtain a hybrid organic-inorganic material used to form pillared and delaminated materials with high accessibility. In contrast, this procedure is still challenging (cost- and time-consuming and with the possible formation of competing mesophases). The separation of individual MWW lamellae was carried out using long alkyl organic molecules (hexadecyltrimethylammonium cations, CTA^+, usually) to populate the interlamellar region. An alkaline media was needed to deprotonate the silanol groups and break the hydrogen bonds between the lamellae. Tetrapropylammonium hydroxide is a double agent because it supplies hydroxide ions and its counter ion (TPA^+) to facilitate the entering of the CTA^+ molecules into the interlamellar region. When NaOH is used, the small Na^+ cations rapidly enter the interlamellar region and compensate negatively charged ions before populating the CTA^+ molecules in the interlamellar region, resulting in an unsuccessfully or partially swollen material [44]. Several studies have sought to better understand swollen materials using different swelling conditions (room temperature or 80 °C), molecular dimensions of swelling agents, hydroxide sources, and strategies of recycling and reusing the swelling solution [45–50].

MCM-36 was the first pillared molecular sieve with zeolite properties. The swollen precursor was mixed with a pillaring agent (TEOS) and went through subsequent calcination where rigid silica pillars

formed, keeping the individual MWW lamella separated from each other. Characterization results showed a surface area of 896 $m^2 \cdot g^{-1}$ (compared with 400 $m^2 \cdot g^{-1}$ for MCM-22) with mesopores between 2 and 4 nm and higher adsorption capacities of bulky molecules as 1,3,5-trimethylbenze (TMB) with 0.040 $mg \cdot g^{-1}$, whereas MCM-22 showed negligible adsorption [51,52].

Another important pillared material was reported, but in this case, aryl silsesquioxane molecules acted as organic pillars between MWW lamellae to obtain a multifunctional organic-inorganic catalytic material with a hierarchical structure [53]. The swollen precursor was reacted with a solution of 1,4-bis(triethoxysilyl)benzene (BTEB) and the CTA^+ molecules were removed by acid extraction. Following this, amino groups were incorporated onto the bridged benzene groups in the interlayer space. The obtained materials showed acid sites provided by the MWW structure of lamellae combined with basic sites from amino groups incorporated on the aryl molecules. Characterization results showed a basal spacing of 4.1 nm, a surface area of 556 $m^2 \cdot g^{-1}$, and a mesoporous region formed by the separated lamellae.

The use of swollen MWW materials treated with ultrasound and acidic medium and a posterior calcination generate ITQ-2, the first delaminated zeolite [54]. Its surface area showed 700 $m^2 \cdot g^{-1}$ and a broad distribution of mesopores due to the random stacking of MWW lamellae in edge-to-face orientation, as shown in Figure 4. ITQ-2 had superior capacities (7 times higher than MCM-22) for the adsorption of TMB and superior catalytic performance for reactions with the cracking of bulky molecules, such as 1,3-diisopropylbenzene and vacuum gas oil in gasoline and diesel [55].

The use of confined subnanometric platinum species was reported and made use of a swelling procedure [56]. In this approach, a solution containing subnanometric platinum species was added during the swelling procedure of the ITQ-1 precursor. After calcination, a three-dimensional zeolite containing platinum confined in the supercavities and on the external surface of the MWW crystallites was formed, as shown in Figure 5. The authors also studied the growth of these platinum species by high-temperature oxidation-reduction treatments, obtaining small nanoparticles with sizes between 1 and 2 nm.

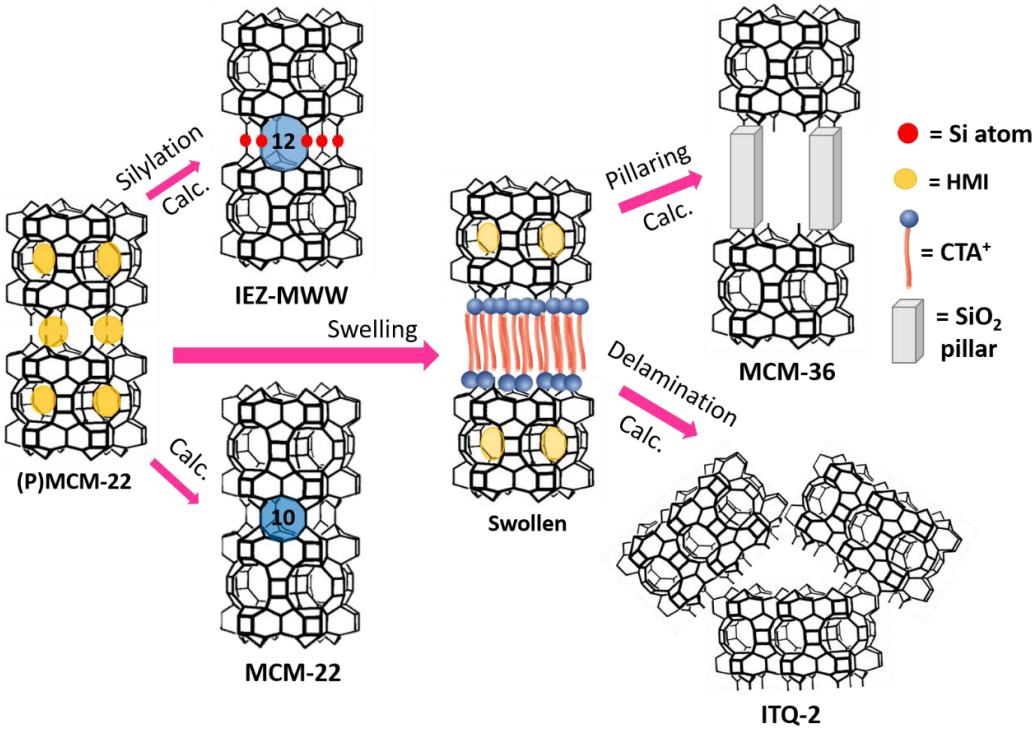

Figure 4. Representation of the postsynthetic procedures to obtain the interlayer expanded zeolite IEZ-MWW, swollen, pillared (MCM-36), and delaminated (ITQ-2) MWW-type materials.

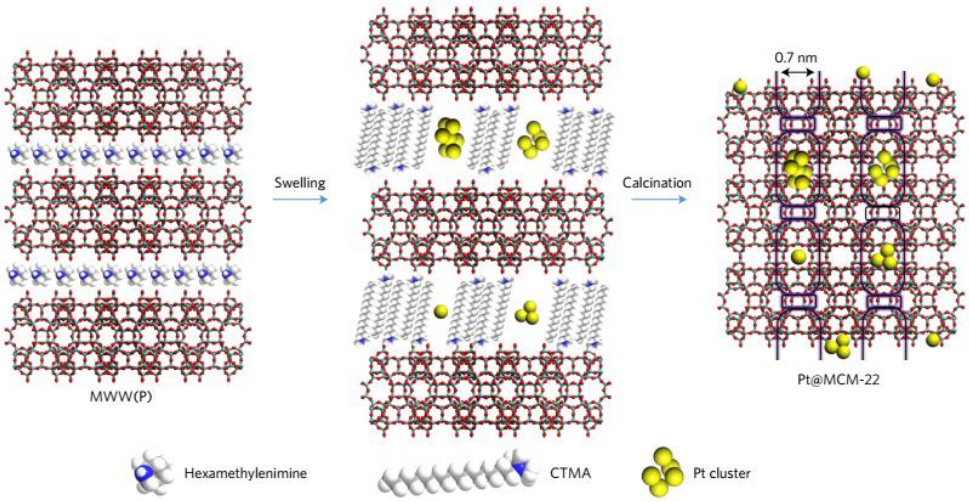

Figure 5. Scheme of confining platinum species in the MCM-22 structure by swelling the MWW precursor with surfactants and platinum species and a subsequent calcination. Reprinted with permission from Springer Nature, Reference [56].

Recently, a novel strategy to obtain delaminated MWW-type zeolite employed a treatment using commercially available telechelic liquid polybutadienes at room temperature and a swollen precursor [57]. The resulting swollen precursor/polymer suspension was subject to ultrasound or a chaotic flow treatment in a planetary mixing system, as shown in Figure 6. The authors confirmed delamination using small angle X-ray scattering (SAXS) results, where no interlamellar reflections were observed using hydroxyl-terminated polybutadiene (HTPB) with 36 min of chaotic flow. On the other hand, the sonication procedure is also effective, but required 5 h to obtain a delaminated material. Another interesting result was the increase in the interlamellar space of the swollen precursor from 4.6 nm to 9.4 nm after manual mixing with HTPB for only 1 min. The authors also pointed out that the end groups of the liquid polybutadienes preferentially interact with the zeolite surface through hydrogen bonds and this is the key factor needed to obtain a delaminated material.

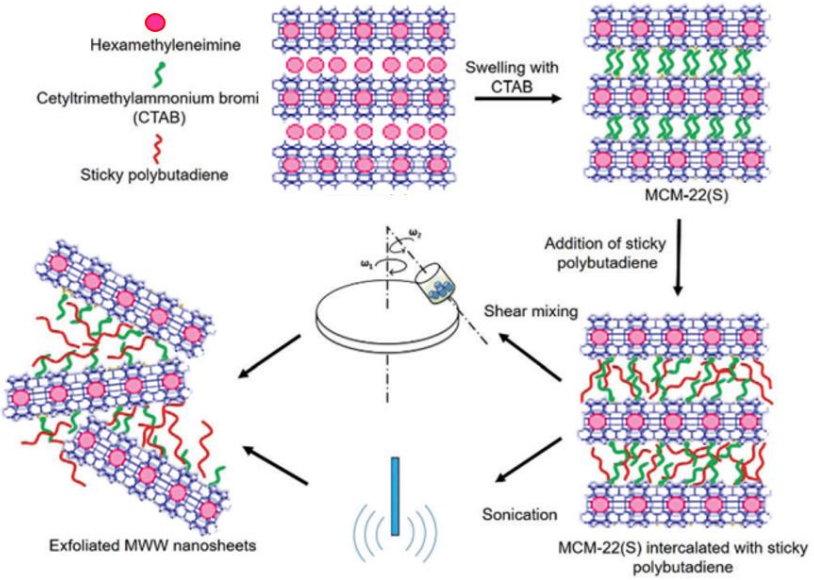

Figure 6. Scheme of the formation of delaminated MWW-type material using telechelic liquid polybutadienes. Adapted from Reference [57]. Copyright (2017), with permission of The Royal Society of Chemistry.

Another post-synthetic approach to obtain more open structures in MWW-type materials is to generate intracrystalline mesopores [41]. This strategy uses MCM-49 zeolite and mixtures of CTA^+ and NaOH under different temperatures and times to obtain desilicated MWW-type materials, as shown in Figure 7. Under the post-synthesis treatment, fragments of the MWW zeolitic structure were removed by the attack of the hydroxide ions in the defects, whereas the CTA^+ molecules acted as a defensive barrier to avoid uncontrollable dissolution by NaOH. Thus, intracrystalline mesopores were formed by the regions where CTA^+ presented "defensive failures." The obtained materials showed a distribution of mesopores with sizes between 2 and 4 nm.

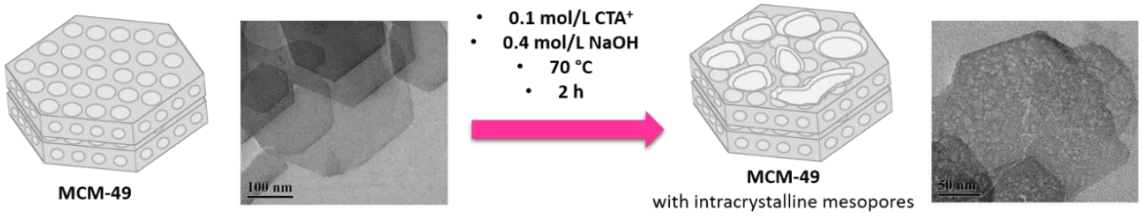

Figure 7. Post-synthesis treatment to obtain intracrystalline mesopores in MCM-49 zeolite. TEM micrographs were taken from Reference [58]. Copyright (2015), with permission from Elsevier.

4. MWW-Type Materials by Direct Synthesis

Several efforts have been made to obtain individual zeolitic lamellae separated by direct synthesis, with the main aim of eliminating the swelling and delamination steps. The first MWW-type material with individual lamellae separated from each other was called Direct Synthesis ITQ-2 (DS-ITQ-2). DS-ITQ-2 was obtained by a very similar traditional synthesis of (P)MCM-22 that was modified using *N*-hexadecyl-*N*′-methyl-DABCO ($C_{16}DC_1$) as a dual template, as shown in Figure 8. DABCO acted as an SDA because of its similarity to HMI, while the tail group (C_{16}) avoided the stacking and growth of the structure along the c-axis. The calcined material showed a surface area of 545 $m^2 \cdot g^{-1}$ and microporous volume of 0.12 $cm^3 \cdot g^{-1}$, which is higher than that of the traditional ITQ-2 (0.08 $cm^3 \cdot g^{-1}$). The pore size distribution showed values in a broad range, which is characteristic of delaminated-type zeolites.

MIT-1 was another MWW-type delaminated material obtained by direct synthesis [59]. However, the organic molecule was the $TMAda^+OH^-$ linked by alkyl chains with four, five, or six carbons and connected with a CTA^+ molecule, as shown in Figure 8. In this case, the adamantylammonium as the head-group acted as an SDA, the linkers acted to stabilize the pore mouth, and the hydrophobic tail of the CTA^+ molecule prevented zeolitic growth along the c-axis. MIT-1 had a surface area higher than 500 $m^2 \cdot g^{-1}$ and a broad distribution of mesopore sizes.

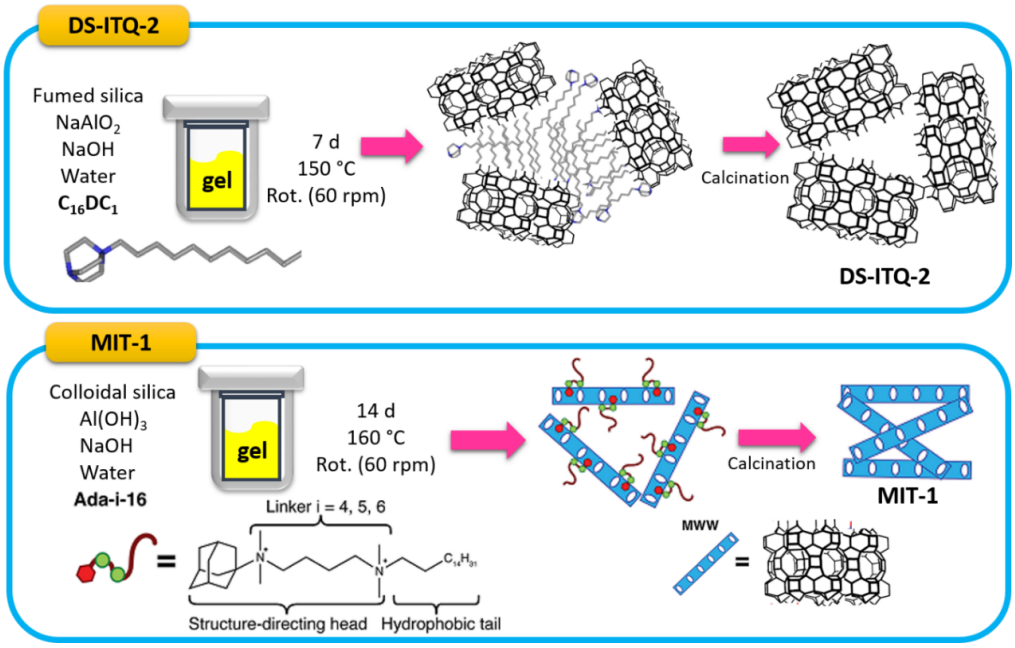

Figure 8. Representation of the syntheses of DS-ITQ-2 and MIT-1.

Both DS-ITQ-2 and MIT-1 are examples of MWW-type materials obtained when the SDA was linked with a long hydrophobic alkyl chain. Another strategy made use of mixtures of SDA and CTA^+ using a dissolution-recrystallization route to obtain a swollen precursor called Al-ECNU-7P by direct crystallization [60]. The synthesis comprises a dissolution containing MWW seeds (ITQ-1), the 1,3-bis(cyclohexyl)imidazolium hydroxide as an SDA, and a silicate source at 140 °C for 1 h followed by the addition of CTA^+ and the aluminum source. Then, the obtained gel was crystallized at 150 °C for 72 h, as shown in Figure 9. From the Al-ECNU-7P, it was possible to obtain a pillared material with a basal spacing of 5 nm, a surface area of 701 $m^2 \cdot g^{-1}$, and a mesopore size distribution centered at 3.1 nm. The direct calcination of Al-ECNU-7P showed delaminated and partially condensed lamellae, a surface area of 502 $m^2 \cdot g^{-1}$, and a mesopore size distribution centered at 5 nm.

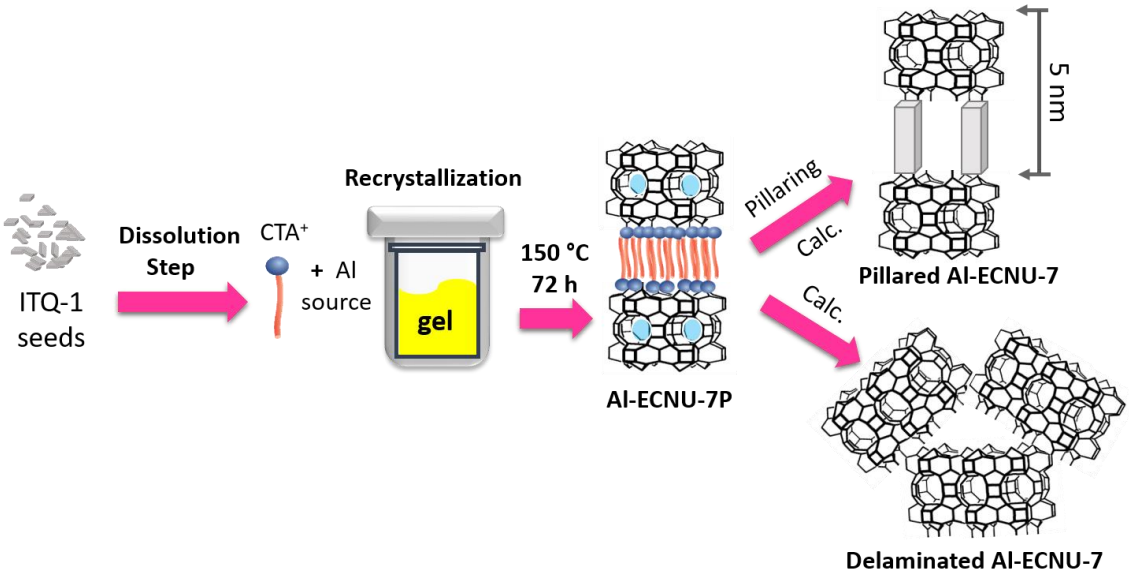

Figure 9. General scheme of the synthesis of Al-ECNU-7P as well as its pillared and delaminated forms.

Another strategy to overcome the diffusional barrier imposed on reactants and products is the synthesis of nanosized zeolites. The decrease of common microsized zeolite crystals to nanosized crystals increases the external surface and could facilitate the rapid diffusion of reactants and products [61]. The synthesis of nanosized MCM-22 zeolite was reported using polydiallydimethylammonium chloride (PDDA) as a protecting or stabilizing agent to avoid the self-aggregation and intergrowth of silica colloids by direct synthesis, as shown in the scheme of Figure 10a. The self-assembly of the cationic polymer and the negatively charged silica species interactions are the main reasons to obtain nanosized MCM-22 with a crystal size of 40 nm, as shown in Figure 10b.

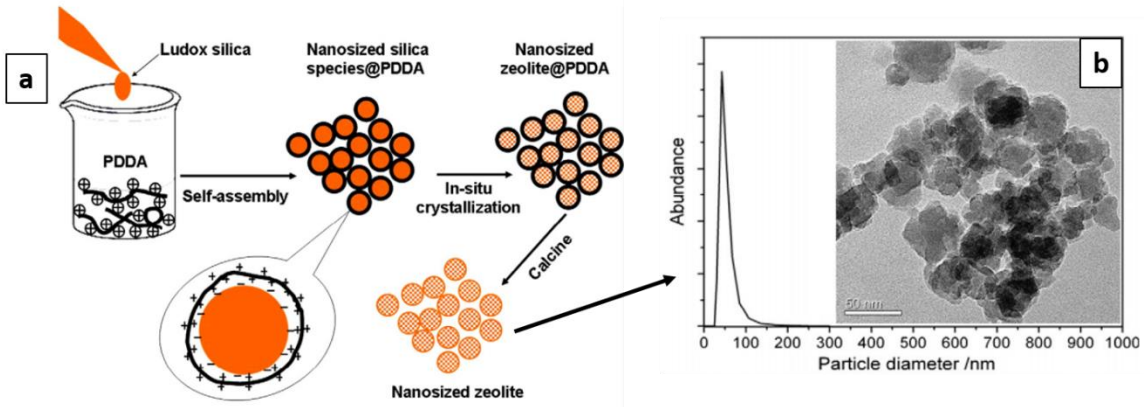

Figure 10. Scheme of the synthesis of nanosized MCM-22 using PDDA (**a**); particle size distribution and TEM of the obtained crystals (**b**). Adapted from Reference [62]. Copyright (2014), with permission from Elsevier.

Recently, a direct synthesis method was reported to obtain dandelion-like MCM-22 microspheres with interparticle meso/macro voids [63]. The authors used carbon black pearls (BP 2000) as a hard template and the synthesis is shown in Figure 11. In the synthesis procedure, colloidal silica was slowly added dropwise to a mixture containing water, sodium aluminate, HMI, and BP 2000 in rotation during nucleation and crystal growth.

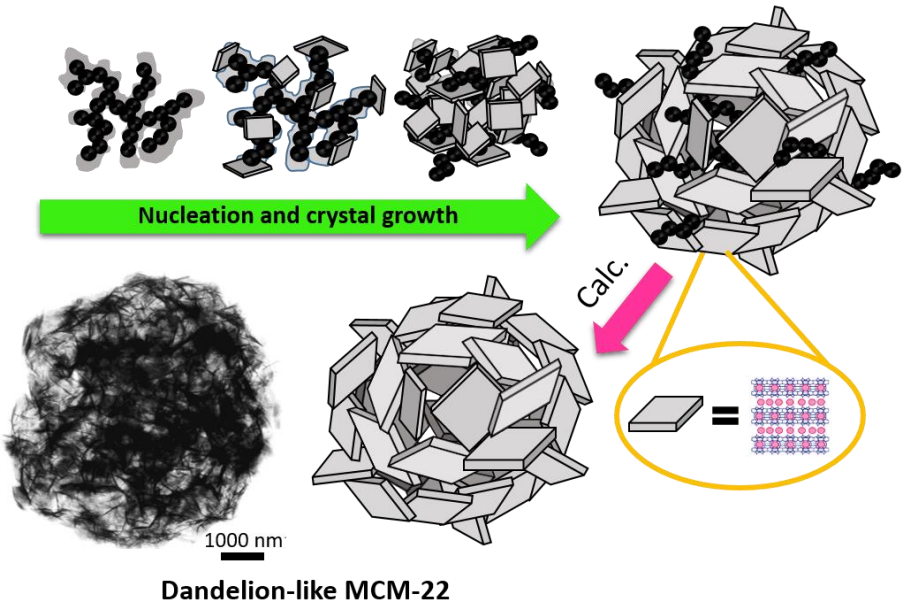

Figure 11. Proposed mechanism of the formation of dandelion-like MCM-22 microspheres. Adapted from Reference [63].

The interactions between BP 2000 and the gel precursor were due to the hydrogen bonds between the functional groups (carboxylic acid, ketone, and ester) present in carbon black and the silanol and amino groups derived from HMI, as well as the Si−O and Al−O bonds. The tortuous shape of BP 2000 aggregates interacts only with the external surfaces of the MWW crystals, forming thin MWW crystal platelets stacked in edge-to-face orientations with interparticle porosity. The pore size distribution showed large mesopores and macropores centered at 200 nm, which is two times higher than that of the traditional MCM-22 zeolite.

5. Conclusions

MWW-type zeolites are attractive nanoporous materials for different applications, due to their three-dimensional and two-dimensional forms. It is interesting that, even 30 years after the discovery of materials with MWW topology, research and development around this family is a matter of continuous interest. Most of this is due to the versatility of the lamellar zeolitic precursor that allows the creation of elegant and different pore architectures with tunable physicochemical properties in terms of acidity, accessibility, and structural stability. The direct synthesis of MWW-type materials with different lamellae organizations are directly linked to the synthesis and discovery of new SDAs with a special attention paid to the dual templates that avoid excessive growth and stacking of the structure along the c-axis. In the future, these routes of synthesis may gain more prominence and extend to other zeolitic structures.

Author Contributions: Conceptualization, A.S; Writing-Original Draft Preparation, A.S and S.P.; Writing-Review & Editing, A.S; Supervision, S.P.

Funding: This research received no external funding.

Acknowledgments: Anderson Schwanke thanks the CAPES Foundation and INOMAT (project number: 88887.136344/2017-00 - 465452/2014-0).

Conflicts of Interest: The authors declare no conflict of interest.

References

1. Tanabe, K.; Hölderich, W.F. Industrial application of solid acid–base catalysts. *Appl. Catal. A Gen.* **1999**, *181*, 399–434. [CrossRef]
2. Vartuli, J.C.; Degnan, T.F., Jr. Applications of mesoporous molecular sieves in catalysis and separations. In *Studies in Surface Science and Catalysis*; Jiří Čejka, H.v.B.A.C., Ferdi, S., Eds.; Elsevier: New York, NY, USA, 2007; Volume 168, pp. 837–854.
3. Corma, A. From Microporous to Mesoporous Molecular Sieve Materials and Their Use in Catalysis. *Chem. Rev.* **1997**, *97*, 2373–2420. [CrossRef] [PubMed]
4. Rinaldi, R.; Schuth, F. Design of solid catalysts for the conversion of biomass. *Energy Environ. Sci.* **2009**, *2*, 610–626. [CrossRef]
5. International Zeolite Association (IZA). Available online: http://www.iza-structure.org/ (accessed on 20 June 2018).
6. Roth, W.J.; Gil, B.; Makowski, W.; Marszalek, B.; Eliasova, P. Layer like porous materials with hierarchical structure. *Chem. Soc. Rev.* **2016**, *45*, 3400–3438. [CrossRef] [PubMed]
7. Diaz, U.; Corma, A. Layered zeolitic materials: An approach to designing versatile functional solids. *Dalton Trans.* **2014**, *43*, 10292–10316. [CrossRef] [PubMed]
8. Roth, W.J.; Cejka, J. Two-dimensional zeolites: Dream or reality? *Catal. Sci. Technol.* **2011**, *1*, 43–53. [CrossRef]
9. Ramos, F.S.O.; de Pietre, M.K.; Pastore, H.O. Lamellar zeolites: An oxymoron? *RSC Adv.* **2013**, *3*, 2084–2111. [CrossRef]
10. Opanasenko, M.V.; Roth, W.J.; Cejka, J. Two-dimensional zeolites in catalysis: Current status and perspectives. *Catal. Sci. Technol.* **2016**, *6*, 2467–2484. [CrossRef]
11. Schwanke, A.J.; Pergher, S. Hierarchical MWW Zeolites by Soft and Hard Template Routes. In *Handbook of Ecomaterials*; Martínez, L.M.T., Kharissova, O.V., Kharisov, B.I., Eds.; Springer: Berlin, Germany, 2017; pp. 1–23.

12. Rubin, M.K.; Chu, P. Composition of Synthetic Porous Crystalline Material, Its Synthesis and Use. U.S. Patent 4954325A, 4 September 1990.
13. Leonowicz, M.E.; Lawton, J.A.; Lawton, S.L.; Rubin, M.K. MCM-22: A Molecular Sieve with Two Independent Multidimensional Channel Systems. *Science* **1994**, *264*, 1910–1913. [CrossRef] [PubMed]
14. Camblor, M.A.; Corma, A.; Díaz-Cabañas, M.-J.; Baerlocher, C. Synthesis and Structural Characterization of MWW Type Zeolite ITQ-1, the Pure Silica Analog of MCM-22 and SSZ-25. *J. Phys. Chem. B* **1998**, *102*, 44–51. [CrossRef]
15. Zhou, D.; Bao, Y.; Yang, M.; He, N.; Yang, G. DFT studies on the location and acid strength of Brönsted acid sites in MCM-22 zeolite. *J. Mol. Catal. A Chem.* **2006**, *244*, 11–19. [CrossRef]
16. Lawton, S.L.; Fung, A.S.; Kennedy, G.J.; Alemany, L.B.; Chang, C.D.; Hatzikos, G.H.; Lissy, D.N.; Rubin, M.K.; Timken, H.-K.C.; Steuernagel, S.; et al. Zeolite MCM-49: A Three-Dimensional MCM-22 Analogue Synthesized by in Situ Crystallization. *J. Phys. Chem. B* **1996**, *100*, 3788–3798. [CrossRef]
17. Bennett, J.M.; Lawton, C.D.C.S.L.; Leonowicz, M.E.; Lissy, D.N.; Rubin, M.K. Synthetic porous crystalline MCM-49, its synthesis and use. U.S. Patent 5236575, 17 August 1993.
18. Fung, A.S.; Lawton, S.L.; Roth, W.J. Synthetic Layered MCM-56, Its Synthesis and Use. U.S. Patent 5362697A, 8 November 1994.
19. Delitala, C.; Alba, M.D.; Becerro, A.I.; Delpiano, D.; Meloni, D.; Musu, E.; Ferino, I. Synthesis of MCM-22 zeolites of different Si/Al ratio and their structural, morphological and textural characterisation. *Microporous Mesoporous Mater.* **2009**, *118*, 1–10. [CrossRef]
20. Ravishankar, R.; Sen, T.; Ramaswamy, V.; Soni, H.S.; Ganapathy, S.; Sivasanker, S. Synthesis, Characterization and Catalytic properties of Zeolite PSH-3/MCM-22. In *Studies in Surface Science and Catalysis*; Weitkamp, J., Karge, H.G., Pfeifer, H., Hölderich, W., Eds.; Elsevier: New York, NY, USA, 1994; Volume 84, pp. 331–338.
21. Corma, A.; Corell, C.; Pérez-Pariente, J.; Guil, J.M.; Guil-López, R.; Nicolopoulos, S.; Calbet, J.G.; Vallet-Regi, M. Adsorption and catalytic properties of MCM-22: The influence of zeolite structure. *Zeolites* **1996**, *16*, 7–14. [CrossRef]
22. Wang, Y.M.; Shu, X.T.; He, M.Y. 02-P-34—Static synthesis of zeolite MCM-22. In *Studies in Surface Science and Catalysis*; Galarneau, A., Fajula, F., Di Renzo, F., Vedrine, J., Eds.; Elsevier: New York, NY, USA, 2001; Volume 135, p. 194.
23. Bevilacqua, M.; Meloni, D.; Sini, F.; Monaci, R.; Montanari, T.; Busca, G. A Study of the Nature, Strength, and Accessibility of Acid Sites of H-MCM-22 Zeolite. *J. Phys. Chem. C* **2008**, *112*, 9023–9033. [CrossRef]
24. Meloni, D.; Laforge, S.; Martin, D.; Guisnet, M.; Rombi, E.; Solinas, V. Acidic and catalytic properties of H-MCM-22 zeolites: 1. Characterization of the acidity by pyridine adsorption. *Appl. Catal. A* **2001**, *215*, 55–66. [CrossRef]
25. Onida, B.; Geobaldo, F.; Testa, F.; Aiello, R.; Garrone, E. H-Bond Formation and Proton Transfer in H-MCM-22 Zeolite as Compared to H-ZSM-5 and H-MOR: An FTIR Study. *J. Phys. Chem. B* **2002**, *106*, 1684–1690. [CrossRef]
26. Güray, I.; Warzywoda, J.; Baç, N.; Sacco, A., Jr. Synthesis of zeolite MCM-22 under rotating and static conditions. *Microporous Mesoporous Mater.* **1999**, *31*, 241–251. [CrossRef]
27. Wu, Y.; Ren, X.; Wang, J. Facile synthesis and morphology control of zeolite MCM-22 via a two-step sol–gel route with tetraethyl orthosilicate as silica source. *Mater. Chem. Phys.* **2009**, *113*, 773–779. [CrossRef]
28. Inagaki, S.; Kamino, K.; Hoshino, M.; Kikuchi, E.; Matsukata, M. Textural and catalytic properties of MCM-22 zeolite crystallized by the vapor-phase transport method. *Bull. Chem. Soc. Jpn.* **2004**, *77*, 1249–1254. [CrossRef]
29. Wu, Y.; Ren, X.; Lu, Y.; Wang, J. Crystallization and morphology of zeolite MCM-22 influenced by various conditions in the static hydrothermal synthesis. *Microporous Mesoporous Mater.* **2008**, *112*, 138–146. [CrossRef]
30. Cheng, Y.; Lu, M.; Li, J.; Su, X.; Pan, S.; Jiao, C.; Feng, M. Synthesis of MCM-22 zeolite using rice husk as a silica source under varying-temperature conditions. *J. Colloid Interface Sci.* **2012**, *369*, 388–394. [CrossRef] [PubMed]
31. Zones, S.I. A crystalline zeolite SSZ-25 Is Prepared Using an Adamantane Quaternary Ammonium Ion as a Template. E.U. Patent 231860, 12 May 1987.
32. Puppe, L.; Weisser, J. Crystalline Aluminosilicate PSH-3 and Its Process of Preparation. U.S. Patent 4439409A, 23 March 1984.

33. Bellussi, G.; Perego, G.; Cierici, M.G.; Giusti, A. Bulletin of the Chemical Society of Japan. E.U. Patent 293032, 30 November 1988.
34. Rohde, L.M.; Lewis, G.J.; Miller, M.A.; Moscoso, J.G.; Gisselquist, J.L.; Patton, R.L.; Wilson, S.T.; Jan, D.Y. Crystalline Aluminosilicate Zeolitic Composition: UZM-8. U.S. Patent 6756030B1, 21 March 2003.
35. Corma, A.; Díaz-Cabanas, M.J.; Moliner, M.; Martínez, C. Discovery of a new catalytically active and selective zeolite (ITQ-30) by high-throughput synthesis techniques. *J. Catal.* **2006**, *241*, 312–318. [CrossRef]
36. Roth, W.J.; Dorset, D.L.; Kennedy, G.J. Discovery of new MWW family zeolite EMM-10: Identification of EMM-10P as the missing MWW precursor with disordered layers. *Microporous Mesoporous Mater.* **2011**, *142*, 168–177. [CrossRef]
37. Zones, S.I.; Davis, T.M. Zeolite SSZ-70 Having Enhanced External Surface Area. E.U. Patent 3027559B1, 30 July 2013.
38. Xu, L.; Ji, X.; Jiang, J.-G.; Han, L.; Che, S.; Wu, P. Intergrown Zeolite MWW Polymorphs Prepared by the Rapid Dissolution–Recrystallization Route. *Chem. Mater.* **2015**, *27*, 7852–7860. [CrossRef]
39. Xing, E.; Shi, Y.; Xie, W.; Zhang, F.; Mu, X.; Shu, X. Synthesis, characterization and application of MCM-22 zeolites via a conventional HMI route and temperature-controlled phase transfer hydrothermal synthesis. *RSC Adv.* **2015**, *5*, 8514–8522. [CrossRef]
40. Xing, E.; Shi, Y.; Xie, W.; Zhang, F.; Mu, X.; Shu, X. Perspectives on the multi-functions of aniline: Cases from the temperature-controlled phase transfer hydrothermal synthesis of MWW zeolites. *Microporous Mesoporous Mater.* **2017**, *254*, 201–210. [CrossRef]
41. Ji, P.; Shen, M.; Lu, K.; Hu, B.; Jiang, J.-G.; Xu, H.; Wu, P. ECNU-10 zeolite: A three-dimensional MWW-Type analogue. *Microporous Mesoporous Mater.* **2017**, *253*, 137–145. [CrossRef]
42. Chu, W.; Li, X.; Liu, S.; Zhu, X.; Xie, S.; Chen, F.; Wang, Y.; Xin, W.; Xu, L. Direct synthesis of three-dimensional MWW zeolite with cyclohexylamine as an organic structure-directing agent. *J. Mat. Chem. A* **2018**. [CrossRef]
43. Wu, P.; Ruan, J.; Wang, L.; Wu, L.; Wang, Y.; Liu, Y.; Fan, W.; He, M.; Terasaki, O.; Tatsumi, T. Methodology for Synthesizing Crystalline Metallosilicates with Expanded Pore Windows Through Molecular Alkoxysilylation of Zeolitic Lamellar Precursors. *J. Am. Chem. Soc.* **2008**, *130*, 8178–8187. [CrossRef] [PubMed]
44. Roth, W.J. Cation Size Effects in Swelling of the Layered Zeolite Precursor MCM-22-P. *Pol. J. Chem.* **2006**, *80*, 703–708.
45. Maheshwari, S.; Jordan, E.; Kumar, S.; Bates, F.S.; Penn, R.L.; Shantz, D.F.; Tsapatsis, M. Layer Structure Preservation during Swelling, Pillaring, and Exfoliation of a Zeolite Precursor. *J. Am. Chem. Soc.* **2008**, *130*, 1507–1516. [CrossRef] [PubMed]
46. Schwanke, A.J.; Pergher, S.; Díaz, U.; Corma, A. The influence of swelling agents molecular dimensions on lamellar morphology of MWW-type zeolites active for fructose conversion. *Microporous Mesoporous Mater.* **2017**, *254*, 17–27. [CrossRef]
47. Chlubná, P.; Roth, W.J.; Zukal, A.; Kubů, M.; Pavlatová, J. Pillared MWW zeolites MCM-36 prepared by swelling MCM-22P in concentrated surfactant solutions. *Catal. Today* **2012**, *179*, 35–42. [CrossRef]
48. Roth, W.J.; Chlubná, P.; Kubů, M.; Vitvarová, D. Swelling of MCM-56 and MCM-22P with a new medium—Surfactant-tetramethylammonium hydroxide mixtures. *Catal. Today* **2013**, *204*, 8–14. [CrossRef]
49. Roth, W.J.; Čejka, J.; Millini, R.; Montanari, E.; Gil, B.; Kubu, M. Swelling and Interlayer Chemistry of Layered MWW Zeolites MCM-22 and MCM-56 with High Al Content. *Chem. Mater.* **2015**, *27*, 4620–4629. [CrossRef]
50. Schwanke, A.J.; Díaz, U.; Corma, A.; Pergher, S. Recyclable swelling solutions for friendly preparation of pillared MWW-type zeolites. *Microporous Mesoporous Mater.* **2017**, *253*, 91–95. [CrossRef]
51. Kresge, C.T.; Roth, W.J.; Simmons, K.G.; Vartuli, J.C. Layered oxide materials and swollen and pillared forms thereof. WO Patent 1992011934A1, 23 July 1992.
52. Roth, W.J.; Kresge, C.T.; Vartuli, J.C.; Leonowicz, M.E.; Fung, A.S.; McCullen, S.B. MCM-36: The first pillared molecular sieve with zeolite properties. In *Studies in Surface Science and Catalysis*; Beyer, H.K., Karge, H.G., Kiricsi, I., Nagy, J.B., Eds.; Elsevier: New York, NY, USA, 1995; Volume 94, pp. 301–308.
53. Corma, A.; Díaz, U.; García, T.; Sastre, G.; Velty, A. Multifunctional Hybrid Organic−Inorganic Catalytic Materials with a Hierarchical System of Well-Defined Micro- and Mesopores. *J. Am. Chem. Soc.* **2010**, *132*, 15011–15021. [CrossRef] [PubMed]
54. Corma, A.; Fornes, V.; Pergher, S.B.C.; Maesen, T.L.M.; Buglass, J.G. Delaminated zeolite precursors as selective acidic catalysts. *Nature* **1998**, *396*, 353–356. [CrossRef]

55. Corma, A.; Diaz, U.; Fornés, V.; Guil, J.M.; Martínez-Triguero, J.; Creyghton, E.J. Characterization and Catalytic Activity of MCM-22 and MCM-56 Compared with ITQ-2. *J. Catal.* **2000**, *191*, 218–224. [CrossRef]
56. Liu, L.; Díaz, U.; Arenal, R.; Agostini, G.; Concepción, P.; Corma, A. Corrigendum: Generation of subnanometric platinum with high stability during transformation of a 2D zeolite into 3D. *Nat. Mat.* **2017**, *16*, 1272. [CrossRef] [PubMed]
57. Sabnis, S.; Tanna, V.A.; Li, C.; Zhu, J.; Vattipalli, V.; Nonnenmann, S.S.; Sheng, G.; Lai, Z.; Winter, H.H.; Fan, W. Exfoliation of two-dimensional zeolites in liquid polybutadienes. *Chem. Commun.* **2017**, *53*, 7011–7014. [CrossRef] [PubMed]
58. Gao, N.; Xie, S.; Liu, S.; Xin, W.; Gao, Y.; Li, X.; Wei, H.; Liu, H.; Xu, L. Development of hierarchical MCM-49 zeolite with intracrystalline mesopores and improved catalytic performance in liquid alkylation of benzene with ethylene. *Microporous Mesoporous Mater.* **2015**, *212*, 1–7. [CrossRef]
59. Luo, H.Y.; Michaelis, V.K.; Hodges, S.; Griffin, R.G.; Roman-Leshkov, Y. One-pot synthesis of MWW zeolite nanosheets using a rationally designed organic structure-directing agent. *Chem. Sci.* **2015**, *6*, 6320–6324. [CrossRef] [PubMed]
60. Xu, L.; Ji, X.; Li, S.; Zhou, Z.; Du, X.; Sun, J.; Deng, F.; Che, S.; Wu, P. Self-Assembly of Cetyltrimethylammonium Bromide and Lamellar Zeolite Precursor for the Preparation of Hierarchical MWW Zeolite. *Chem. Mater.* **2016**, *28*, 4512–4521. [CrossRef]
61. Mintova, S.; Grand, J.; Valtchev, V. Nanosized zeolites: Quo Vadis? *C. R. Chim.* **2016**, *19*, 183–191. [CrossRef]
62. Yin, X.; Chu, N.; Yang, J.; Wang, J.; Li, Z. Synthesis of the nanosized MCM-22 zeolite and its catalytic performance in methane dehydro-aromatization reaction. *Catal. Commun.* **2014**, *43*, 218–222. [CrossRef]
63. Schwanke, A.; Villarroel-Rocha, J.; Sapag, K.; Díaz, U.; Corma, A.; Pergher, S. Dandelion-Like Microspherical MCM-22 Zeolite Using BP 2000 as a Hard Template. *ACS Omega* **2018**, *3*, 6217–6223. [CrossRef] [PubMed]